"Mircea cel Batran" Naval Academy Scientific Bulletin, Volume XVIII – 2015 – Issue 2
Published by "Mircea cel Batran" Naval Academy Press, Constanta, Romania // The journal is indexed in:
PROQUEST SciTech Journals, PROQUEST Engineering Journals, PROQUEST Illustrata: Technology, PROQUEST Technology Journals, PROQUEST Military Collection PROQUEST Advanced Technologies & Aerospace

CFD MODELLING OF A 5 BLADED PROPELLER BY USING THE RANSE APPROACH

Marian RISTEA[1]
Adrian POPA[2]
Dragos Ionut NEAGU[3]
[1]Assist. prof. PhD, eng "Mircea cel Batran" Naval Academy, Marine Engineering and Naval Weapons Department
[2]Assist. prof. PhD, eng "Mircea cel Batran" Naval Academy, Marine Engineering and Naval Weapons Department
[3]PhD attendee, S.C. Marine and Offshore Consultants S.R.L., Constanta, Romania

Abstract: *Computational fluid dynamics (CFD) represents a branch of fluid mechanics that uses algorithms, numerical methods and computers in order to simulate various processes associated to flow conditions. In this manner, the flow developed in naval propellers is simulated by using a number of conservation equations together with several additional equations, models for turbulence, pressure, cavitation, heat exchange and chemical species transport or dispersed phases equations.*
Keywords: *CFD; simulation; mesh; Navier - Stokes equations; turbulence modeling; fluid continuity; momentum conservation*

Introduction

Computational Fluid Dynamics, or CFD, is the computational technology for the analysis of systems involving fluid flow, heat transfer and associated phenomena by means of computer - based simulation. This technology employs numerical methods and algorithms to solve the equations that describe fluid flows and heat transfer. Computers are used to prepare the data, build computational domain and mesh, perform numerical solution of the equations, and to analyze the solution results.

The equations that are describing the dynamics of fluid represent fundamental laws of physics stating conservation of mass, momentum and energy. Thus, CFD is intended to model realistic media and various bodies interacting with it by virtual (non-physical) means, and to predict their behavior under different conditions. In other words, CFD enables scientists and engineers to perform "numerical experiments" (i.e. computer-based simulations) in a "virtual laboratory".

Nowadays CFD methods are routinely used in a wide range of industrial and nonindustrial application areas. These areas include, for example:

- Aerodynamics of aircraft and space vehicles (prediction of lift and drag, and airflow analysis);
- Ship and propeller hydrodynamics (prediction of resistance, propeller characteristics, cavitation, maneuvering forces);
- Marine engineering (estimation of wind, wave and current loads on offshore structures);
- Power plant technological processes (combustion processes in engine and gas turbines, functions of cooling systems);
- Turbo machinery (analysis of flow in rotating blade-row passages and diffusers, cavitation);
- Chemical process engineering (studies on chemical reactions, mixing, separation, polymer molding);
- Architecture and building construction (calculation of wind loads on buildings, design of heating, ventilation, water supply and sewage systems); Environmental engineering (analysis of distribution of pollutants and effluents);
- Hydrology and oceanography (studies on flows in rivers, estuaries, oceans);
- Meteorology (weather prediction and long term climate forecasting);
- Biomedical engineering (modeling of blood flows through arteries and veins).

Analysis of motion of a fluid element

When deriving the equations of fluid motion, we need to know rate of change of a fluid property φ per unit mass and per unit volume. Following the method by Euler we will investigate the field of φ (*x*, *y*, *z*, *t*) assuming that the property of interest is the function of the position of the fluid particle and time. At the given time instant *t* the particle was located at the point (*x*, *y*, *z*), and after one time step *t*+Δ*t* it moved to another point with the coordinates (*x*+Δ*x*, *y*+Δ*y*, *z*+Δ*z*).

The rate of change of property φ per unit volume is given by the product of substantial derivative and density:

$\frac{\partial \rho}{\partial t} + \nabla(\rho \vec{U}) = 0$, where ρ -water density,

$\vec{U}$ = (u,v,w) - fluid velocity

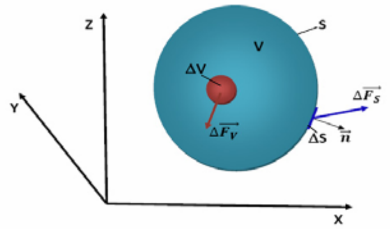

Figure 1. Surface and body forces acting on a fluid volume

The obtained relationship between the substantive derivative of a fluid property, which follows a fluid particle, and the rate of change of this property for a fluid element is fundamental for the derivation and analysis of the *governing equations of fluid motion*, which represent mathematical expressions of the *conservation laws* of physics. These laws are:

• The mass of fluid is conserved (continuity equation).

• The rate of change of momentum equals the sum of the forces acting on a fluid particle (Newton's second law).

• The rate of change of energy equals the sum of the rate of heat addition to and rate of work done on a fluid particle (first law of thermodynamics).

Navier-Stokes equations for momentum conservation

Viscous stresses in the momentum equations can be related to the rates of linear deformations of the fluid element, and the latter are expressed through the velocity components. For the isotropic Newtonian fluids, the relationship between the stresses and rates of deformations is given by the following equation:

$$\begin{vmatrix} p_{xx} & \tau_{xy} & \tau_{xz} \\ \tau_{yx} & p_{yy} & \tau_{yz} \\ \tau_{zx} & \tau_{zy} & p_{zz} \end{vmatrix} = -\begin{vmatrix} p & 0 & 0 \\ 0 & p & 0 \\ 0 & 0 & p \end{vmatrix} + 2\mu \cdot \begin{vmatrix} \varepsilon_x & \vartheta_z & \vartheta_y \\ \vartheta_z & \varepsilon_y & \vartheta_x \\ \vartheta_y & \vartheta_x & \varepsilon_z \end{vmatrix}$$

This is the form of momentum equations that is the most convenient for the finite volume method formulation. In some sources, the name Navier-Stokes equations is associated with the system of momentum equations and continuity equation.

Turbulence Phenomenon

As a physical phenomenon, turbulence may or may not be desirable. Below we will give just a few examples illustrating the opposite effects of turbulence:

• Intensive mixing between the zones with different momentum content can be useful in industrial chemical or thermal mixing processes.

• In the external flows around ships, airplanes and cars, the increased mixing of momentum results in increased frictional forces and, hence, higher skin friction component of drag, compared to laminar flows. At the same time, the boundary layer separation is delayed in turbulent flows as the separation point moves further downstream, and, as a result, the form drag is reduced.

• Atmospheric turbulence caused by mixing of warm and cold air by wind must be accounted for the safe operation of aircraft; it can represent a serious risk factor depending on intensity of turbulence and size of the aircraft.

• Large scale turbulence plays an important role in formation of oceanic currents and atmospheric circulation that can influence weather condition and even climate over large areas.

• Dispersion and mixing of pollutants and contaminants in rivers, seas and atmosphere are dependent on turbulence mechanisms.

In CFD, the random nature of turbulent flows complicates their numerical simulation greatly. Extensive theoretical and experimental research on the mechanisms of turbulence has resulted in a truly impressive bibliography on the subject. These complex topics are beyond the scope of the present course. It is however important to understand the physics and key features of turbulent flow as these underlay the concepts of numerical modeling.

Classification and understanding of turbulence modeling concepts

Numerical modeling of turbulence represents a very challenging task which requires deep understanding of the physics of turbulent flows and extensive knowledge of mathematical methods. In this paper we will approach the practical implications of the modeling approaches. We will begin with a general classification of turbulence modeling concepts, which according to (Bardina et al, 1980) can be divided into the six categories:

1. Concept using correlations: These methods allow for obtaining simple formulas for the hydrodynamic characteristics as functions of the modeling criteria that are valid for simple flows, e.g. Prandtl-Schlichting formula for the skin friction of a flat plate in turbulent flow or ITTC-57 model-ship correlation line.

2. Concept using integral equations: The integral equations are derived from the general equations of motion by integrating them over one or more coordinates. This approach is used, for example, in solution of boundary layer equations discussed. The problem is reduced to one or more ordinary differential equations which are easier to solve than partial differential equations, but the range of validity of this approach is limited.

3.One-point closure concept: These methods use time-averaging and ensemble-averaging of the equations of motion, such as we have considered in the previous section. The averaging leads to a set of partial differential equations called Reynolds-Averaged Navier-Stokes (RANS) equations which represent the main tool in the arsenal of CFD methods used nowadays for the engineering computations of turbulent flows. The averaging makes the equations simpler, but at the same time introduces additional unknowns. In order to form a closed set of equations, the introduction of turbulence models is needed. The purpose of a turbulence model is to relate the additional unknowns that characterize transport of the turbulence properties to the averaged properties of the mean flow.

4. Two-point closure concept: The approach is

based on use of the equations for correlation of the velocity components at two points in space or the Fourier transformation of these equations. Two-point closure methods are mainly used for the modeling of homogeneous turbulence and they have not found wide practical application.

5.Large Eddy Simulation (LES) concept: LES methods provide solution for the largest scale motions of turbulent flow. In other words, the largest – and energetically most important – turbulent eddies are computed directly, while the effect of smaller eddies, which are not resolved, is accounted for through additional stresses obtained from the turbulence theory.

6. Direct Numerical Simulation (DNS) concept: DNS methods solve the Navier-Stokes equations directly for all scales of turbulent motions.

Reynolds Averaged Navier-Stokes equations (RANSE)

The equations of the RANS method for incompressible viscous flow are derived by averaging of the Navier-Stokes equations (2). We will only consider the time averaging of the instantaneous continuity and momentum equation. The velocity vector, velocity components and pressure are presented as a superposition of the mean and fluctuations parts:

$$u = \bar{u} + u'$$
$$v = \bar{v} + v'$$
$$w = \bar{w} + w'$$

The density and viscosity of fluid are constant, and the additional momentum sources do not contain fluctuating part. The averaging rules for the mean and fluctuating parts are applied.

It has to be noted that, after averaging, all the same terms are present in the momentum equation, now referring to the mean values. However, one additional term appeared as a result of averaging of the convective term. This new term constitutes convective momentum transfer due to turbulent fluctuations of velocity. It is common to place this term in the right-hand side of the equation to reflect its effect as an additional turbulent stress component on the mean velocity component.

Analogous derivations can be done for the y and z momentum equations, and we arrive at the following set of equations for momentum:

$$\frac{\partial(\rho u)}{\partial t} + \nabla(\rho u \vec{U}) = -\frac{\partial p}{\partial x} + \frac{\partial \tau_{xx}}{\partial x} + \frac{\partial \tau_{yx}}{\partial y} + \frac{\partial \tau_{zx}}{\partial z} + \rho F_x$$
$$\frac{\partial(\rho v)}{\partial t} + \nabla(\rho v \vec{U}) = -\frac{\partial p}{\partial x} + \frac{\partial \tau_{xy}}{\partial x} + \frac{\partial \tau_{yy}}{\partial y} + \frac{\partial \tau_{zy}}{\partial z} + \rho F_y$$
$$\frac{\partial(\rho w)}{\partial t} + \nabla(\rho w \vec{U}) = -\frac{\partial p}{\partial x} + \frac{\partial \tau_{xz}}{\partial x} + \frac{\partial \tau_{yz}}{\partial y} + \frac{\partial \tau_{zz}}{\partial z} + \rho F_z$$

The equations depicted above are called *Reynolds-Averaged Navier-Stokes Equations*, and they represent the main set of equations to be solved in the RANSE method. In order to close the set of RANS equations, one has to relate turbulent stresses to mean velocity components. The complex nature of turbulence does not allow for simple relations between the fluctuating and mean velocity components.

The aforementioned relations are established by turbulence models which may vary greatly in complexity of formulation depending on what effects and to what extent these turbulence models are intended to include.

Turbulence models in RANSE simulation

We have now approached one of the most difficult topics in CFD which is related to modeling of turbulence. From the observations after the simplest turbulent flows we have made in the previous sections one can conclude that it is highly unlikely that one can expect a single turbulence model to be universally suitable for all classes of problems studied, with the exception of DNS modeling which is so far too expensive to be of practical engineering use. Indeed, the choice of turbulence model will depend on such considerations as flow physics, best practice for a specific class of flows, desired levels of accuracy and, of course, available computational resources and time. In view of the limited volume of the present course, the accent will be made on understanding of the key features of the main turbulence models currently used with RANSE simulations and implications of their practical use, rather than their numerical implementation in solution algorithms.

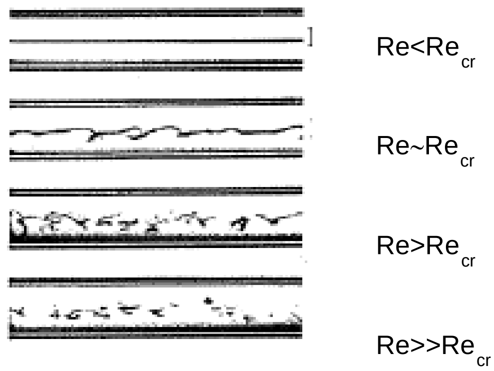

Figure 2. ***Re_{cr}*** **– critical Reynolds number when instability of the flow causes the growth of vortical structures and their chaotic motion – turbulence**

The most common turbulence models for RANSE simulation can be classified following the scheme presented in Table 1.

Table 1. Classification of turbulence models used in RANSE simulations

Class	Group	Turbulence
Zero-equation models	Mixing length model	Isotropic turbulence
One-equation model	Spalart-Allmaras model	Isotropic turbulence
Two-equation model	k-ε models	Isotropic turbulence
	k-ω models	Isotropic turbulence
	v^2-f models	Anisotropic

		turbulence
Reynolds stress equation models	RSM	Anisotropic turbulence
Algebraic stress models	ASM	Anisotropic turbulence
Coupled models	DES	Anisotropic turbulence

CFD study of a naval five bladed propeller

In order to develop the CFD study for a naval propeller, there was chosen the five bladed propeller, developed for the Workshop on Verification and Validation of Maneuvering Simulation Methods held in Copenhagen, Denmark, in 14th – 16th of April 2008, by Maritime and Ocean Engineering Research Institute (MOERI), Korea. The KCS was conceived to provide data for both explication of flow physics and CFD validation for a modern container ship with bulb bow and stern (i.e., ca. 1997).

The conditions include bare hull and fixed model. No full-scale ship exists. More information concerning KCS including towing tank results for resistance, generated wave field and pressure field on the hull can be found on the MOERI and NMRI web sites.

The study presented in the following pages was carried in the CAE laboratory from „Mircea cel Batran" Naval Academy, using Ansys CFX 12.1.

The geometry of the propeller is presented in figure 3.

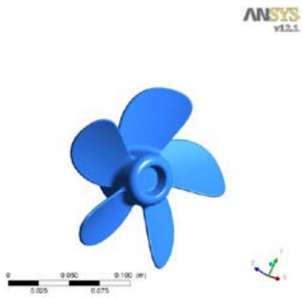

Figure 3 – The geometry for the MOERI KCS propeller

The geometry's parameters, developed by the main contributors to the conference (NMRI – Japan, MOERI – Korea and SVA – Germany) are presented in Table 2.

Table 2. Geometry parameters

Model built by	not built	MOERI	SVA	NMRI
Tested at	n.a.	MOERI (PMM)	SVA (free), CEHIPAR (PMM, BSHC (free), FHR (shallow)	NMRI (CMT)
Scale	1.000	31.599	52.667	75.500
Propeller				
Type	FP	FP	CP	FP
No. of blades	5	5	5	5

During the stages necessary to develop the simulation it was obtained an unstructured mesh with 400760 nodes and 2164604 elements, represented in figures 4 and 5.

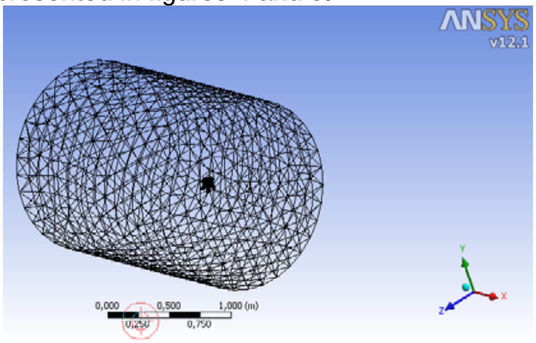

Figure 4 – Domain mesh

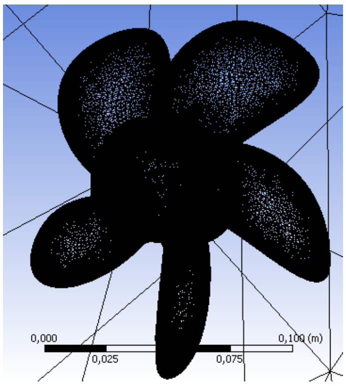

Figure 5 – Mesh refinement on the propeller's surface

The initial data used for the domain's definition are presented in table 3.

Table 3 – Domain's boundary settings (excerpt from the Ansys 12.1 analysis report)

Boundaries	
Boundary - inlet	
Settings	
Flow Regime	Subsonic
Mass And Momentum	Cartesian Velocity Components
U	-2.5000e+00 [m s^-1]
V	0.0000e+00 [m s^-1]
W	0.0000e+00 [m s^-1]
Turbulence	High Intensity and Eddy Viscosity Ratio
Boundary - outlet	
Settings	
Flow Regime	Subsonic
Mass And Momentum	Average Static Pressure
Pressure Profile Blend	5.0000e-02
Relative Pressure	1.0000e+00 [atm]
Pressure Averaging	Average Over Whole Outlet

Boundary - propeller	
Type	WALL
Settings	
Mass And Momentum	No Slip Wall
Wall Roughness	Smooth Wall
Boundary - wall	
Settings	
Mass And Momentum	Free Slip Wall

After establishing the settings for the boundaries, there were carried 2 different types of simulations. The first one was a static simulation, where the flow is fully developed and $t \rightarrow 0$. The second simulation was a transient simulation, developed on a certain time frame, of 500 seconds, with 5 seconds timesteps and 3 iterations per timestep.
In the 4th table there are presented the results for the first simulation,

Table 4 - Forces and Torques for static simulation

Location	**Type**	**X**	**Y**	**Z**
Propeller	Pressure Force	-4.2401e+01	-1.0000e-01	-2.8792e-02
	Viscous Force	-5.8192e-02	1.2704e-03	4.8602e-03
	Total Force	-4.2459e+01	-9.8730e-02	-2.3932e-02
	Pressure Torque	-1.2847e+00	2.7848e-03	-4.6414e-03
	Viscous Torque	9.6976e-05	-1.4184e-04	5.0230e-05
	Total Torque	-1.2846e+00	2.6430e-03	-4.5912e-03

Table 5. Forces and Torques for transient simulation

Location	**Type**	**X**	**Y**	**Z**
Propeller	Pressure Force	-4.243e+01	-8.978e-02	7.303e-02
	Viscous Force	-5.494e-02	8.326e-03	-3.089e-03
	Total Force	-4.248e+01	-8.146e-02	6.994e-02
	Pressure Torque	-1.288e+00	-9.035e-04	-9.721e-03
	Viscous Torque	-5.265e-05	8.171e-05	1.325e-04
	Total Torque	-1.288e+00	-8.218e-04	-9.589e-03

We can see that the values calculated for the same parameters are different between the two simulations. The values deviation related to the static simulation are presented in the 6th table.

Table 6 – Values deviation for the calculated parameters

Location	Type	X	Y	Z
Propeller	Pressure Force	0%	-10%	-354%
	Viscous Force	-6%	555%	-164%
	Total Force	0%	-17%	-392%
	Pressure Torque	0%	-132%	109%
	Viscous Torque	-154%	-158%	164%
	Total Torque	0%	-131%	109%

These differences are established due to the convergence criteria and because in the first simulation, the static one, the flow is related to an indefinite period of time; on the other hand, in the transient simulation case, the flow is defined for a specific period of time.
In the following figures are presented the charts for pressure and velocity development during the simulation in several reference planes (xOy and xOz).

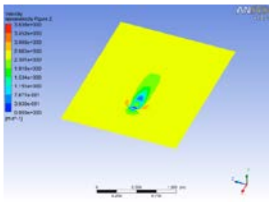

Figure 6 - The velocity in horizontal place – static simulation

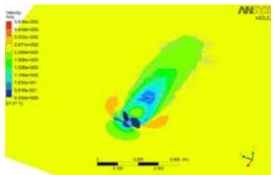

Figure 7 - The velocity in horizontal place – transient simulation

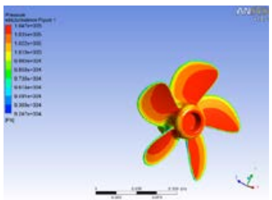

Figure 8 – Pressure profile on the propeller's surface – static simulation

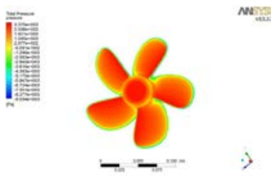

Figure 9 – Pressure profile on the propeller's surface place – transient simulation

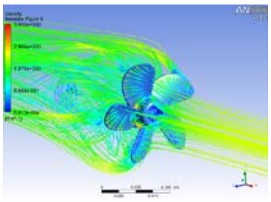

Figure 10 – Flow development – static simulation

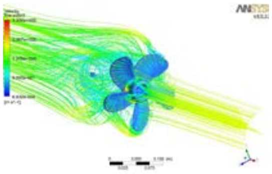

Figure 11 – Flow development – transient simulation

CONCLUSIONS

After analyzing the results deviation and the graphical results, we can conclude that the velocity and pressure fields will develop by following the same patterns for each type of simulation. The flow development – streamlines will have also the same shape for each case.

When we are thinking at results, we can observe large deviations between the two particular cases, but we can’t state which is right or wrong, due to the initial premises assumed for the simulation cases.

As a conclusion, because the flow over the propeller geometry is a very complicated problem, the best results will be considered to be the results determined by the transient simulation. Also, the static simulation, also known as Steady State simulation can be used, in this particular situation, to validate the settings for boundaries and to verify the meshing system.

BIBLIOGRAPHY:

[1] Van, S.H., Kim, W.J., Kim, D.H., Yim, G.T., Lee, C.J., and Eom, J.Y., 1997, "Measurement of Flows Around a 3600TEU Container Ship Model," Proceedings of the Annual Autumn Meeting, SNAK, Seoul, pp. 300-304 (in Korean).

[2] Lee, J., Lee, S.J., and Van, S.H., 1998, "Wind Tunnel Test on a Double Deck Shaped Ship Model," 3rd International Conference on Hydrodynamics, Seoul, Korea.

[3] Van, S.H., Kim, W.J., Yim, G.T., Kim, D.H., and Lee, C.J., 1998, "Experimental Investigation of the Flow Characteristics Around Practical Hull Forms," Proceedings 3rd Osaka Colloquium on Advanced CFD Applications to Ship Flow and Hull Form Design, Osaka, Japan

[4] Fujisawa, J., Ukon, Y., Kume, K., and Takeshi, H., "Local Velocity Field Measurements around the KCS Model (SRI M.S.No.631) in the SRI 400m Towing Tank," Ship Performance Division Report No. 00-003-02, The Ship Research Institute of Japan, April 27, 2000. SPD Report No. 00-003-02

[5] Tsukada, Y., Hori, T., Ukon, Y., Kume, K., and Takeshi, H., SPD Report No. 00-004-01

[6] Kume, K., Ukon, Y., Fujisawa, J., Hori, T., Tsukada, Y., and Takeshi, H., "Uncertainty Analysis for the KCS Model (SRI M.S.No.631) Test in the SRI 400m Towing Tank," Ship Performance Division Report No. 00-008-01, The Ship Research Institute of Japan, June 1, 2000. SPD Report No. 00-008-01

[7] www.simman2008.dk